

Prospects for MSSM Higgs Searches at the Tevatron

Patrick Draper^{a,c}, Tao Liu^a, and Carlos E.M. Wagner^{a,b,c}

^a Enrico Fermi Institute and ^b Kavli Institute for Cosmological Physics,
University of Chicago, 5640 S. Ellis Ave., Chicago, IL 60637

^c HEP Division, Argonne National Laboratory, 9700 Cass Ave., Argonne, IL 60439

Abstract

We analyze the Tevatron reach for neutral Higgs bosons in the Minimal Supersymmetric Standard Model (MSSM), using current exclusion limits on the Standard Model Higgs. We study four common benchmark scenarios for the soft supersymmetry-breaking parameters of the MSSM, including cases where the Higgs decays differ significantly from the Standard Model, and provide projections for the improvements in luminosity and efficiency required for the Tevatron to probe sizeable regions of the $(m_A, \tan \beta)$ plane.

1 Introduction

The minimal supersymmetric Standard Model (MSSM) is an ultraviolet completion of the Standard Model (SM) that provides a technical solution to the hierarchy problem, is consistent with the unification of gauge couplings at high energies, and includes a natural dark matter candidate [1]. The model includes two Higgs doublets, and for supersymmetric particle masses smaller than about 1 TeV, contains in most of the parameter space a Higgs with SM-like couplings to the vector gauge bosons and a mass that is smaller than about 130 GeV [2],[3],[4],[5],[6],[7],[8]. The MSSM also contains non-standard CP-even and CP-odd neutral Higgs bosons, which present enhanced couplings to the down quarks and SM charged leptons relative to the couplings of the SM Higgs. Probing the MSSM Higgs sector therefore demands a combination of SM-like as well as non-standard Higgs boson searches.

Possible searches for SM-like Higgs bosons at the Tevatron colliders have been analyzed in the literature [9],[10],[11],[12],[13],[14],[15],[16],[17],[18]. Recently, the CDF and $D\bar{0}$ collaborations released a combined analysis of the Tevatron search for the Higgs boson in the Standard Model, resulting in the exclusion of the SM Higgs at 95% C.L. in the mass range 160-170 GeV and improved bounds on the Higgs production cross section in the lower mass range [19]. The inclusion of multiple Higgs production and decay channels in the analysis was crucial in obtaining the new limits, particularly in the low-mass region.

Some Higgs searches at the Tevatron, particularly in the $\tau^+\tau^-$ channel, have already sought Higgs bosons with non-SM-like gauge couplings directly [20],[21],[22],[23],[24],[25],[26]. These limits are relevant for the search for non-standard Higgs bosons in the MSSM. In the following, we will consider the limits from these searches independently before combining them with the limits from the SM-like Higgs searches, and find a complementarity in the coverage of MSSM parameter space.

In this note, we quantify the improvements in luminosity and signal efficiency necessary for the Tevatron to place exclusion limits on the Higgs sector of the MSSM. We begin in section 2 by reviewing briefly the MSSM Higgs spectrum and the coupling strengths relative to the Standard Model. Then, in section 3 we discuss the translation of Standard Model exclusion limits into limits on the MSSM. We examine four benchmark scenarios in the MSSM parameter space and analyze the limit-setting potential of the Tevatron according to a range of increases in luminosity and efficiencies projected by the experimental collaborations. If the experiments can achieve these improvements, we find that it will have significant exclusion coverage of the MSSM Higgs sector parameter space. Moreover, even parameter regions previously considered inaccessible to the Tevatron due to a suppression of the branching fraction of $h \rightarrow b\bar{b}$ appear accessible through the $h \rightarrow W^+W^-$ channel. For convenience, all figures presented in this paper are available online at <http://home.uchicago.edu/~pdraper/MSSMHiggs/MSSMHiggs.html>. We summarize our conclusions in section 4.

2 MSSM Higgs Spectrum and Couplings

The Higgs sector of the MSSM consists of two complex scalar doublets H_1 and H_2 , which present tree-level couplings to only down-type quarks and up-type quarks respectively. CP is conserved in the tree-level scalar potential, so the neutral fields split into two CP -even mass eigenstates h and H and one CP -odd mass eigenstate A . The CP -even mass matrix at tree level is given in the (H_1, H_2) basis by

$$\mathcal{M}^2 = \begin{pmatrix} m_A^2 \sin^2 \beta + m_Z^2 \cos^2 \beta & -(m_A^2 + m_Z^2) \sin \beta \cos \beta \\ -(m_A^2 + m_Z^2) \sin \beta \cos \beta & m_A^2 \cos^2 \beta + m_Z^2 \sin^2 \beta \end{pmatrix}. \quad (2.1)$$

The CP -odd mass m_A and $\tan \beta$, the ratio of the vacuum expectation values of the neutral components of the two Higgs doublets, are inputs of the tree level mass matrix. \mathcal{M}^2 can be diagonalized by introducing a mixing angle α :

$$\begin{pmatrix} h \\ H \end{pmatrix} = \begin{pmatrix} -\sin \alpha & \cos \alpha \\ \cos \alpha & \sin \alpha \end{pmatrix} \begin{pmatrix} H_1^0 \\ H_2^0 \end{pmatrix}. \quad (2.2)$$

At tree level, the mass of the lightest CP -even eigenstate h is bounded, $m_h \leq m_Z$. As emphasized before, if the soft supersymmetry-breaking mass scale is $M_S \simeq 1$ TeV, radiative corrections can lift the bound to $m_h \lesssim 130$ GeV. In the limit of large m_A (the decoupling limit, in which h has SM-like couplings) and keeping only contributions proportional to α_3 and the top Yukawa, the two-loop analytic formula for m_h reads [3]

$$m_h^2 = m_Z^2 \cos^2 2\beta \left(1 - \frac{3}{8\pi^2} \frac{m_t^2}{v^2} t \right) + \frac{3}{4\pi^2} \frac{m_t^4}{v^2} \left[\frac{1}{2} X_t + t + \frac{1}{16\pi^2} \left(\frac{3}{2} \frac{m_t^2}{v^2} - 32\pi\alpha_3 \right) (X_t t + t^2) \right], \quad (2.3)$$

where

$$X_t = \frac{2a_t^2}{M_S^2} \left(1 - \frac{a_t^2}{12M_S^2} \right) \quad (2.4)$$

and

$$t = \log \frac{M_S^2}{m_t^2}. \quad (2.5)$$

In Eq. (2.4), a_t is the stop squark mixing parameter given by $a_t \equiv A_t - \mu/\tan \beta$, where A_t is the soft trilinear stop parameter and μ is the Higgsino mass parameter. The running parameters α_3 and m_t are evaluated at the scale of the top quark mass. From this formula it is clear that the upper bound on m_h is achieved for large $\tan \beta$ in the ‘‘maximal mixing’’ scenario, where $a_t = \sqrt{6}M_S$.

The mixing angle α satisfies the tree level relation

$$\frac{m_A^2 + m_Z^2}{m_A^2 - m_Z^2} \cdot (\cot \alpha - \tan \alpha) = (\cot \beta - \tan \beta), \quad (2.6)$$

where $-\frac{\pi}{2} \leq \alpha \leq 0$. Assuming CP conservation, the couplings of the CP -even Higgs h and H to gauge bosons are given by the Standard Model couplings multiplied by $\sin(\beta - \alpha)$ and $\cos(\beta - \alpha)$, respectively. The tree level couplings of h and H to down-type fermions are the Standard Model Yukawa couplings multiplied by $-\sin \alpha / \cos \beta$ and $\cos \alpha / \cos \beta$ respectively, and the couplings to up-type fermions are similarly rescaled by $\cos \alpha / \sin \beta$ and $\sin \alpha / \sin \beta$.¹ This implies that for associated production of h with a W boson,

$$\frac{\sigma_{MSSM}}{\sigma_{SM}} = \sin^2(\beta - \alpha), \quad (2.7)$$

whereas for the production of h via gluon fusion through a loop of top quarks,

$$\frac{\sigma_{MSSM}}{\sigma_{SM}} \approx \frac{\cos^2 \alpha}{\sin^2 \beta}. \quad (2.8)$$

The latter ratio is only valid in the limit of heavy superpartners, because it ignores the possible contribution of squark loops. In our analysis we will instead use the fact that the gluon fusion cross section is directly proportional to the Higgs decay to gg :

$$\frac{\sigma_{MSSM}}{\sigma_{SM}} = \frac{\Gamma_{MSSM}(h \rightarrow gg)}{\Gamma_{SM}(h \rightarrow gg)}. \quad (2.9)$$

3 Constraints and the R Parameter in the Standard Model

The plots produced by CDF and DØ ([29],[30]) provide upper limits at 95% C.L. on the parameter $R_{SM,i}$, which is the Higgs signal in the decay channel i , normalized to the signal in that channel predicted by the Standard Model:

$$R_{SM,i} \equiv \frac{\sigma_i Br_i}{\sigma_{SM,i} Br_{SM,i}}. \quad (3.10)$$

Naïve estimates for the limits are obtained by assuming no signal is seen and the errors are only statistical:

$$R_{SM,i}^{95} \equiv 1.96 \times \frac{\sqrt{b_i}}{s_{SM,i}}, \quad (3.11)$$

where $s_{SM,i}$ and b_i are the expected signal and background from the SM in the i th channel. An upper limit derived from the combination of all channels is also provided by the experimental collaborations [29],[31]. $R_{SM,comb}$ is defined to be the Higgs signal in

¹For large values of $\tan \beta$, the down-type quark couplings are affected by loop corrections that may be of $\mathcal{O}(1)$ [27] and alter the production cross sections and branching ratios of the non-standard Higgs bosons in a significant way [23],[28].

all channels normalized to the predicted SM signal, and therefore parametrizes a space of theories that differ from the SM only by a universal rescaling of all production cross sections. Its 95% C.L. upper limit $R_{SM,comb}^{95}$ can be reproduced to good approximation by combining Gaussian errors from each channel:

$$\begin{aligned}
R_{SM,comb}^{95} &= 1.96 \times \frac{\sqrt{b_{comb}}}{s_{SM,comb}} \\
&= 1.96 \times \frac{1}{\sqrt{\sum_i \frac{(s_{SM,i})^2}{b_i}}} \\
&= \frac{1}{\sqrt{\sum_i \frac{1}{(R_{SM,i}^{95})^2}}}.
\end{aligned} \tag{3.12}$$

To illustrate the effectiveness of this approximation, in Figs. 1 and 2 we show the R_{SM}^{95} curves from individual channels and the combined constraints as presented by CDF and DØ. We include the following search channels: $h \rightarrow b\bar{b}$ with the Higgs produced in association with W or Z bosons, the $h \rightarrow \tau^+\tau^-$ inclusive search, and the $gg \rightarrow h \rightarrow W^+W^-$ search. For each experiment we overlay the combined curve obtained from Eq. (3.12), and find that it is in good agreement with the combined result presented by each collaboration. In Fig. 3, we combine the results from CDF and DØ, again comparing with the overall combined curve given by the collaborations [19]. Note that with these curves, the mass range 160–170 GeV is not excluded. This is because we are combining the *expected* limits from each channel, rather than the experimentally observed limits. A downward fluctuation was observed in the analysis of the $h \rightarrow W^+W^-$ channel, leading to the exclusion. The reason we take the expected limits is so that we can rescale them by projected increases in luminosity and signal efficiency. The overall SM Higgs limits corresponding to three such improvement scenarios are also presented in Fig. 3. The first assumes an increase in luminosity up to 10 fb^{-1} per experiment in all channels. Such an increase in luminosity is expected, if the Tevatron continues running until mid-2011. The second assumes the same luminosity increase, as well as 25% efficiency improvements in the detection of the $b\bar{b}$ and W^+W^- Higgs decay channels. The final scenario increases the efficiency improvements further to 50%. It is important to note that each of these efficiency improvements scale down the previous upper bound by about 20%. This is approximately the same reduction achieved by increasing the luminosity from 7 fb^{-1} to 10 fb^{-1} , or by decreasing the statistical significance from 95% to 90%. Therefore, our results can be reinterpreted in this context: if the luminosity only reaches 7 fb^{-1} , an efficiency improvement of 50% in the $b\bar{b}$ and W^+W^- channels will be necessary to reach the exclusion limit achieved with 10 fb^{-1} and a 25% increase in efficiency. If only 25% is gained in efficiency and 7 fb^{-1} in luminosity, the same exclusions will apply at 90% C.L.

We emphasize that our naïve combination leads to a conservative upper limit on the R parameter, up to about 10% larger than that presented by the experimental collaborations in some ranges of Higgs mass. Furthermore, it does not include the

possible effects of new search channels. For example, one channel not included in our analysis is the $h \rightarrow \gamma\gamma$ from $D\theta$, which, from the results of Ref. [32], would improve the naïve combined bound on R by up to 1.5% in the 120–140 GeV mass range. Therefore, our improvement factors imply upper bounds on those required for large coverage of the SM Higgs mass range.

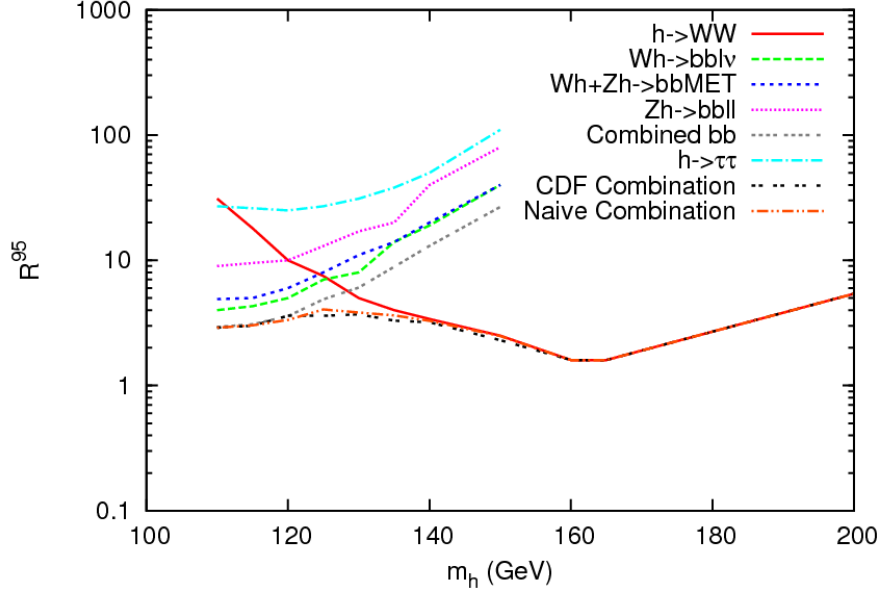


Figure 1: Individual channel and combined constraints on R_{SM} at 95% C.L. from CDF. The orange curve gives the naïve analytic combination.

It is clear from Figs. 1- 3 that Higgs masses near 125 GeV will be the most difficult to probe. It is essential in this region to include constraints from both $b\bar{b}$ and W^+W^- decay channels. As a test of the strength of the W^+W^- limit in the low mass region, in Fig. 4 we plot the limit in the SM and in a modification of the SM where the Higgs coupling to down-type fermions is highly suppressed, leading to an enhancement of the branching ratio to W^+W^- . This scenario arises in a certain window of MSSM parameters. We can see from Fig. 4 that the bound is quite strong ($R^{95} \lesssim 2$ for $120\text{GeV} \lesssim m_h \lesssim 170\text{GeV}$) even without any improvements in efficiency or luminosity.

4 The R Parameter in the MSSM

The combined constraint cannot be used immediately to place limits on the MSSM, because as mentioned previously it is a constraint on models that differ from the SM by a single constant rescaling of $\sigma \times Br$ for all channels. In the MSSM, different channels will be related to the SM channels by different rescalings. Therefore, each channel should

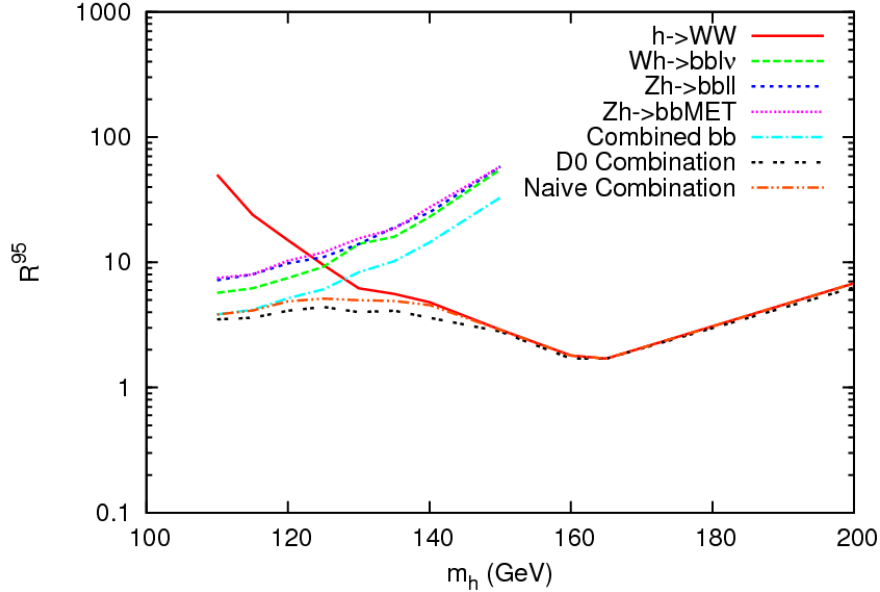


Figure 2: Individual channel and combined constraints on R_{SM} at 95% C.L. from $D\emptyset$. The orange curve gives the naïve analytic combination.

be individually scaled so that the R^{95} constraint bounds the Higgs signal normalized to the expected signal from the MSSM:

$$R_{MSSM,i}^{95} = R_{SM,i}^{95} \times \frac{\sigma_{SM,i} Br_{SM,i}}{\sigma_{MSSM,i} Br_{MSSM,i}}. \quad (4.13)$$

Then, the $R_{MSSM,i}^{95}$ can be combined as in Eq. (3.12) above to give a net constraint on the MSSM.

We include both the light and the heavy CP -even MSSM Higgs bosons as intermediate states for each channel. The most sensitive Tevatron searches for SM-like Higgs bosons have been in the $b\bar{b}$ channel with associated production of the Higgs, and the W^+W^- channel with Higgs production via gluon fusion. These channels require sizeable Higgs gauge couplings, and therefore have been primarily relevant for the light Higgs h , which has SM-like gauge couplings in most of parameter space. However, as m_A decreases the mixing angle becomes larger and m_H becomes smaller, so H becomes increasingly SM-like and consequently plays a bigger role in the constraints inferred from these searches.

In contrast to $b\bar{b}$, the $\tau^+\tau^-$ channel search is inclusive [33], and therefore conservative limits can be inferred for both SM-like and nonstandard Higgs searches. As an upper limit on the associated production channel, it can be interpreted as a constraint from an SM-like search. This constraint is typically quite weak compared to the limit from the $b\bar{b}$ channels, as can be seen from Fig. 1 and assuming the rescaling factor in Eq. (4.13) is

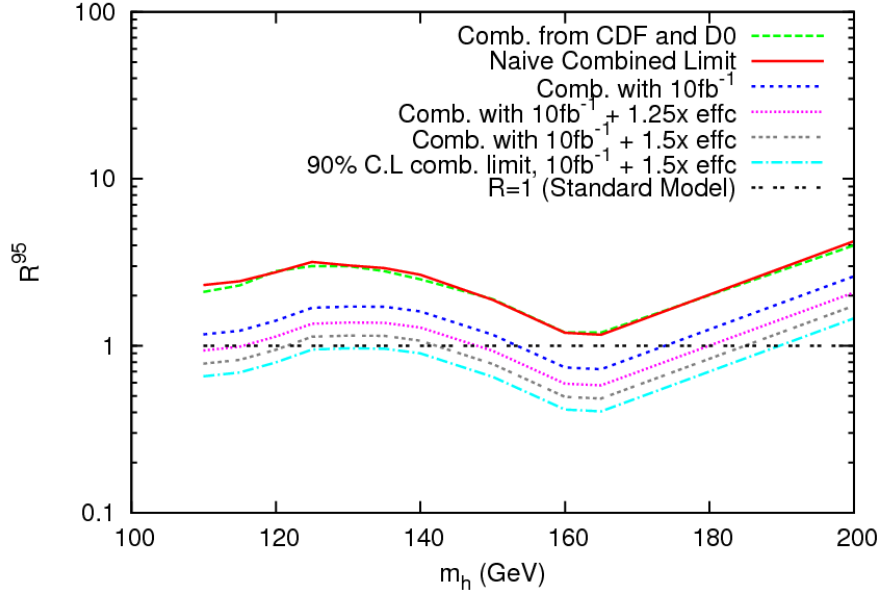


Figure 3: Combined constraints on R_{SM} at 95% C.L. from CDF, $D\emptyset$, and the combination of the two. Also presented are projected limits after increasing the luminosity to 10 fb^{-1} and including 25-50% efficiency improvements.

$\mathcal{O}(1)$. In the following we will always lump this SM-like $\tau^+\tau^-$ constraint together with the $b\bar{b}$ constraint. On the other hand, when the $\tau^+\tau^-$ data is taken as a limit on the gluon fusion production channel, the constraint from the CP-odd and nonstandard CP-even Higgs bosons can be quite strong [25],[26]. These particles have $\tan^2 \beta$ enhanced production rates through loops of bottom quarks, and so the rescaling factor relative to the SM can be significant if they are sufficiently light. In the following, when we refer to the $\tau^+\tau^-$ constraint, we mean this constraint coming from the nonstandard Higgs search.

Our strategy will be as follows: we pick benchmark scenarios for all the MSSM parameters except for $\tan \beta$ and m_A , which are the dominant parameters affecting the Higgs signal. We scan over the $(m_A, \tan \beta)$ plane, calculating the spectrum and the scaling factors $\sigma_{SM,i} Br_{SM,i} / (\sigma_{MSSM,i} Br_{MSSM,i})$ for all channels. The masses and branching ratios are computed numerically using HDECAY [34], and in particular the numerator is calculated at the Standard Model Higgs mass equal to the mass of the CP-even MSSM Higgs in the intermediate state (we checked that similar results are obtained by using CPsuperH [35]). Finally we read off the expected $R_{SM,i}^{95}$ from the CDF and $D\emptyset$ plots and use Eqs. (4.13) and (3.12) to compute the value of R^{95} at each point in the parameter space.

As emphasized before, we will first present our results for the constraints from the SM-like Higgs search channels and the $gg \rightarrow h, H \rightarrow \tau^+\tau^-$ nonstandard search channel

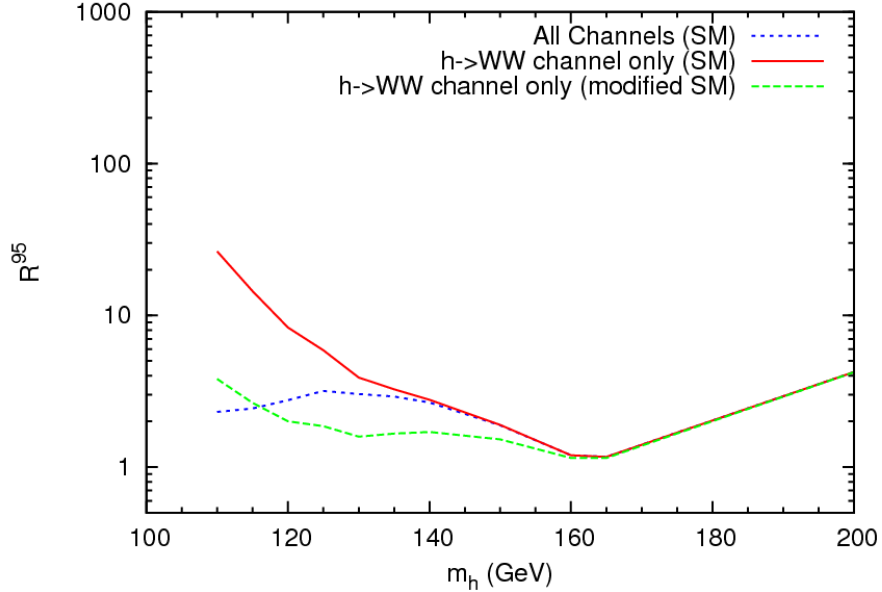


Figure 4: The bound on R at 95% C.L. from the $h \rightarrow W^+W^-$ channel in the SM and in a modified SM scenario where the coupling of h to down-type fermions is suppressed. The combined constraint from all channels is shown for reference.

separately. This will demonstrate the capabilities of the separate searches in covering the MSSM parameter space. At the end we will combine the constraints to see the complementarity of the coverage.

5 Benchmark Scenarios

We consider four benchmark sets of soft parameters [36], which enter in the dominant loop corrections to the Higgs mass matrix. All soft sfermion masses are set to a common value M_S and the top quark mass is set to the current central value of 173.1 GeV [37]. We scan over m_A from 100 GeV to 300 GeV in 100 steps, and $\tan\beta$ from 3 to 60 also in 100 steps. The first benchmark point is the case of maximal mixing, with

$$\begin{aligned}
 M_S &= 1 \text{ TeV}, & a_t &= \sqrt{6}M_S, \\
 \mu &= 200 \text{ GeV}, & M_2 &= 200 \text{ GeV}, \\
 A_b &= A_t, & m_{\tilde{g}} &= 0.8M_S.
 \end{aligned}$$

As mentioned previously, this choice of parameters leads to the largest radiative addition to the lightest Higgs mass. The second point is the opposite scenario of minimal stop

mixing,

$$\begin{aligned} M_S &= 2 \text{ TeV}, & a_t &= 0, \\ \mu &= 200 \text{ GeV}, & M_2 &= 200 \text{ GeV}, \\ A_b &= A_t, & m_{\tilde{g}} &= 0.8M_S. \end{aligned}$$

Here the mass of the lightest Higgs is lower, $m_h \sim 113 - 118$ GeV, and the constraint will be stronger, as can be seen from the Standard Model combined curve. The soft supersymmetry-breaking mass scale is increased in this scenario in order to avoid LEP bounds [38]. We chose a value of μ of order m_Z . A larger value of μ , of the order of the stop masses, would lead to a decrease in the lightest CP-even Higgs mass of about 2 GeV in most of the parameter space, without affecting the quality of Higgs searches in the analyzed channels.

The third benchmark lies in the “gluophobic” region, where the gluon fusion mechanism for production of the SM-like Higgs is suppressed by a cancellation between the top quark loop and the stop loop [39]. This requires a light stop², which can be achieved for a smaller scale M_S and moderate, negative values of the parameter a_t controlling the stop mixing. For this point, we take

$$\begin{aligned} M_S &= 350 \text{ GeV}, & a_t &= -770 \text{ GeV}, \\ \mu &= 300 \text{ GeV}, & M_2 &= 300 \text{ GeV}, \\ A_b &= A_t, & m_{\tilde{g}} &= 500 \text{ GeV}. \end{aligned}$$

The final point is in the “small α_{eff} ” scenario, where μ and A_t take typical intermediate magnitudes but opposite signs. In this case the branching fraction of $h \rightarrow b\bar{b}$ becomes highly suppressed for a certain range of m_A and $\tan\beta$, due to a cancellation in the off-diagonal component of the neutral CP-even Higgs boson mass matrix between tree-level terms suppressed by $1/\tan\beta$ and loop corrections suppressed by factors of $1/(16\pi^2)$. Without an off-diagonal term in the mass matrix, the lightest CP-even Higgs becomes entirely up-type, and does not couple to bottom quarks at tree level (a small coupling appears at the loop-level [23]). The cancellation can be seen explicitly from the loop-corrected off-diagonal matrix element,

$$\begin{aligned} \mathcal{M}_{12}^2 &\simeq - \left[m_A^2 + m_Z^2 - \frac{h_t^4 v^2}{8\pi^2} (3\bar{\mu}^2 - \bar{\mu}^2 \bar{A}_t^2) \right] \sin\beta \cos\beta \\ &+ \left[\frac{h_t^4 v^2}{16\pi^2} \bar{\mu} \tilde{a}_t (\bar{A}_t \tilde{a}_t - 6) \sin^2\beta + \frac{3h_t^2 m_Z^2}{32\pi^2} \bar{\mu} \tilde{a}_t \right] \left[1 + \frac{t}{16\pi^2} (4.5h_t^2 - 0.5h_b^2 - 16g_3^2) \right]. \end{aligned} \quad (5.14)$$

Here h_t and h_b are Yukawa couplings, g_3 is the strong running coupling, $\tilde{a}_t = a_t/M_S$, $\bar{\mu} = \mu/M_S$, $\bar{A}_t = A_t/M_S$, and $t = \log(M_S^2/m_t^2)$. For moderate to large $\tan\beta$, \mathcal{M}_{12}^2

²For an analysis of Tevatron Higgs searches for an alternative MSSM scenario associated with electroweak baryogenesis (in which a light stop enhances gluon fusion), see [40].

vanishes if the following approximate relationship holds:

$$\left[\frac{m_A^2}{m_Z^2} - \frac{1}{2\pi^2}(3\bar{\mu}^2 - \bar{\mu}^2 \bar{A}_t^2) + 1 \right] \simeq \frac{\tan \beta}{150} \left[\bar{\mu} \bar{A}_t (2\bar{A}_t^2 - 11) \right]. \quad (5.15)$$

In the maximal mixing case, this relation cannot be satisfied, and in the no-mixing case, it can only be satisfied for very large $\bar{\mu}$. On the other hand, if $\mu = -A_t \sim M_S$ the relation can be easily satisfied for low m_A . The benchmark values are³

$$\begin{aligned} M_S &= 800 \text{ GeV}, & a_t &= -1.5 \text{ TeV}, \\ \mu &= 1.5 \text{ TeV}, & M_2 &= 500 \text{ GeV}, \\ A_b &= A_t, & m_{\tilde{g}} &= 500 \text{ GeV}. \end{aligned}$$

Fig. 5 demonstrates the suppression of the $b\bar{b}$ branching fractions of the light and heavy Higgs bosons, and Fig. 6 shows the corresponding increase in the branching fractions to W^+W^- . The apex of the cones is the point where the mass eigenvalues become degenerate, and so the mixing angle and consequently the cross sections and decay widths vary rapidly in the $(m_A, \tan \beta)$ parameter space.

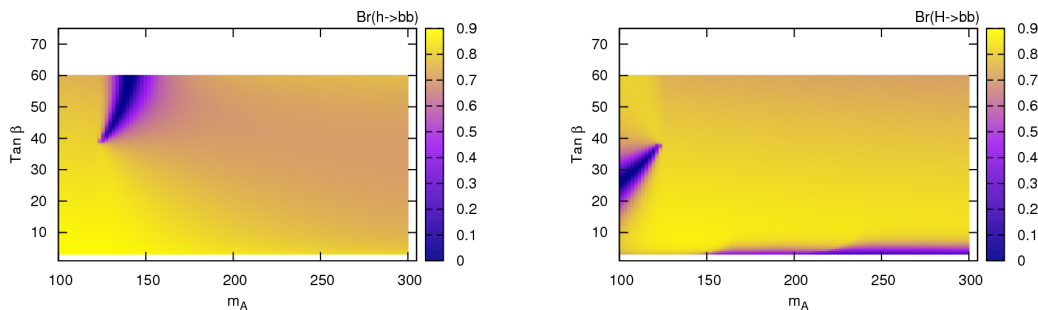


Figure 5: (1) $\text{Br}(h \rightarrow b\bar{b})$ and (2) $\text{Br}(H \rightarrow b\bar{b})$ in the small α_{eff} scenario.

6 Projections and Analysis

Following Eq. (3.11), R^{95} scales inversely the square root of the luminosity and inversely with the signal efficiency. We study the improvements necessary for the Tevatron to exclude regions of MSSM parameter space at 90% and 95% C.L. As in the SM case discussed above, we take as milestones total luminosities of 10 fb^{-1} per experiment

³The values of a_t and μ chosen here differ from those presented in the small- α_{eff} scenario of Ref. [36]. The values here allow a greater contribution to the limit from the WW decay modes of the SM-like Higgs in the regions where its $b\bar{b}$ mode is suppressed. All figures including those corresponding to the benchmark values in [36] are available on the website listed in the introduction.

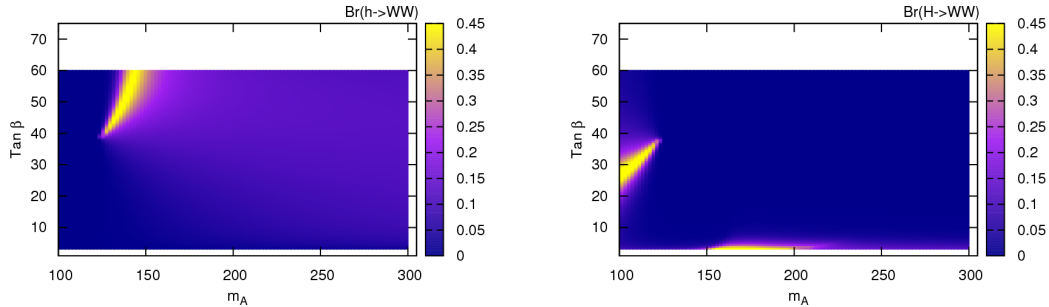


Figure 6: (1) $\text{Br}(h \rightarrow W^+W^-)$ and (2) $\text{Br}(H \rightarrow W^+W^-)$ in the small α_{eff} scenario.

in all channels, and improvement factors of 1.0, 1.25, and 1.5 in the signal efficiency in the $b\bar{b}$ and W^+W^- channels. We assume no efficiency improvement in the $\tau^+\tau^-$ non-standard Higgs boson searches.

Fig. 7 gives the projected limits from the $b\bar{b}$ and W^+W^- channels in the maximal mixing scenario. For large values of $m_A \gg m_Z$, H decouples, and the couplings of h approach the Standard Model values. In this regime h is mostly up-type as α becomes small and negative, but the mixing angle suppression of the coupling to down-type quarks is compensated by the $\tan\beta$ enhancement of the Yukawa. The lightest CP-even Higgs mass in the decoupling limit is close to 125 GeV, which as observed before, is the most difficult mass range for SM-like Higgs bosons searches at the Tevatron collider (see Fig. 3). Hence, large improvements in efficiencies and luminosity will be necessary to probe this scenario.

For moderate, fixed m_A and decreasing $\tan\beta$, the coupling of h to down-type quarks is enhanced by a more rapid increase in $\sin\alpha$ than in $\cos\beta$. Consequently the constraints are stronger than in the SM. At lower values of $m_A \gtrsim m_h$, this effect becomes more pronounced, so a large area can be excluded at 95% C.L. As m_A becomes equal to or smaller than about 125 GeV, however, $\alpha \lesssim -\frac{\pi}{4}$ and the production rate of h by standard processes, which involve couplings to gauge bosons and to the top quark, is substantially decreased for moderate to large $\tan\beta$. Fortunately, in this region m_H is light ($m_H \approx 126$ GeV) and its production rate by standard processes is growing as the production of h falls. The combination of constraints from h and H still produces a moderate exclusion limit in a significant region of the parameters.

In Fig. 8 we present the limits coming only from the $\tau^+\tau^-$ channel search for the nonstandard Higgs. In the low m_A and large $\tan\beta$ regime, h has suppressed gauge couplings and is dominantly down-type. It exchanges this role with H as m_A increases towards the decoupling limit. In either case the nonstandard Higgs is light enough to be produced, mainly by gluon fusion through b and \tilde{b} loops. Its coupling to down-type fermions is enhanced by $\tan\beta$, so the constraint can be significant without any improvements in efficiency or luminosity. The mass and fermionic couplings of the CP-

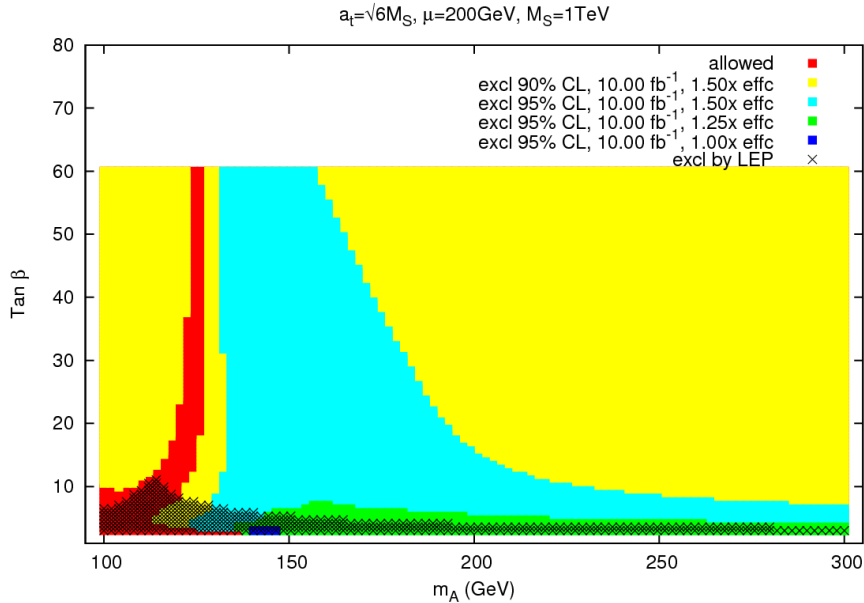


Figure 7: Exclusion limits at 90% and 95% C.L. in the maximal mixing scenario of the MSSM, including only $b\bar{b}$ and W^+W^- decay channels.

odd Higgs A mimic those of the nonstandard Higgs, so we take $2 \times \sigma \times Br$ to approximate its contribution to the $\tau^+\tau^-$ constraint, which, as has been shown in Ref. [41], is only weakly dependent on the value of the soft breaking parameters [27]. In the intense coupling regime, $m_A \sim m_h \sim m_H$, both H and h have sizeable down-type components, leading to the strongest constraints from $\tau^+\tau^-$. Fig. 9 presents the combined limits from both the SM-like and nonstandard Higgs searches. We see that much of parameter space requires a 50% signal efficiency improvement in the $b\bar{b}$ and W^+W^- channels in order to make a test this scenario at the 90% C.L.. The decoupling limit, where h is indistinguishable from a 125 GeV SM Higgs, is the most difficult to probe.

Fig. 10 gives the projected limits from the $b\bar{b}$ and W^+W^- channels in the no-mixing scenario. The behavior of the production and couplings is similar, but smaller loop corrections from the squark sector reduce m_h to around 117 GeV in most of parameter space. These small Higgs boson masses are characteristic of constrained models of supersymmetry, like the CMSSM, in which the A_t parameter is rarely larger than the characteristic stop masses. The constraints are stronger than in the maximal mixing case due to the decrease of R_{SM}^{95} (for a previous analysis in the CMSSM, based on somewhat more optimistic projections of the reach in the $b\bar{b}$ channel, see, for example, Ref. [42]). The black contours in Fig. 10 show the regions of maximal statistical significance that can be achieved in SM-like searches with the full 50% efficiency improvements. Fig. 11 gives the constraints from only the $\tau^+\tau^-$ channel, and Fig. 12 gives the combined limit. We see that all of parameter space can be covered at 95% C.L. if the total integrated

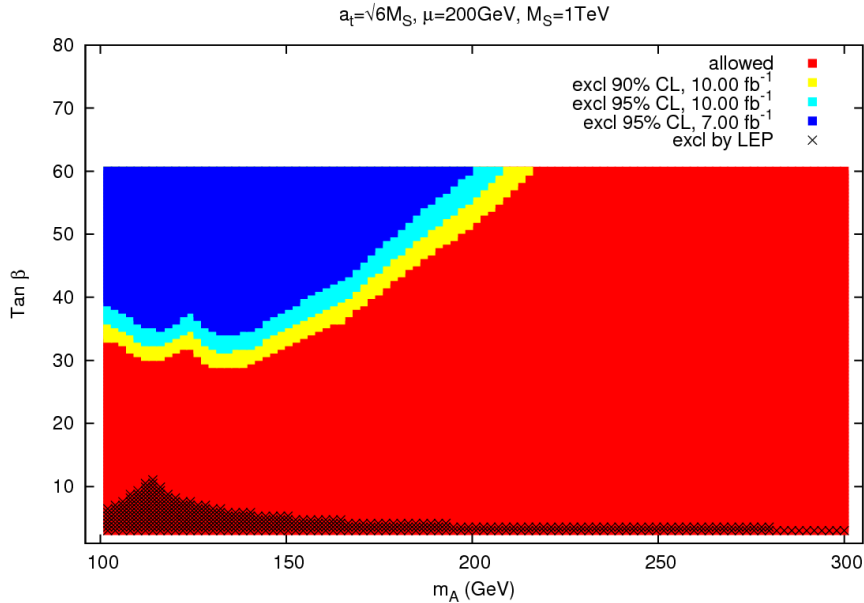


Figure 8: Exclusion limits at 90% and 95% C.L. in the maximal mixing scenario of the MSSM, including only the $\tau^+\tau^-$ inclusive search. No efficiency improvements are applied.

luminosity increases to 10 fb^{-1} and there are 25% efficiency improvements in the SM-Higgs search channels.

Fig. 13 gives the projected limits from the $b\bar{b}$ and W^+W^- channels in the gluophobic region. The suppression of gluon fusion spoils the utility of the $h \rightarrow W^+W^-$ channel, but the SM-like Higgs mass is lower and so the $b\bar{b}$ constraints are dominant. This leads to a result qualitatively very similar to what we found in the no-mixing scenario. Fig. 14 gives the limits from just the $\tau^+\tau^-$ channel, which are again similar to the no-mixing case because gluon fusion production of the nonstandard Higgs bosons, which is governed by down-type quark and squark loops, is not suppressed. There is a feature at $m_A \simeq 260$ GeV which is caused by the opening of the $H \rightarrow \tilde{t}_1\tilde{t}_1^*$ decay channel, where $m_{\tilde{t}_1} \simeq 130$ GeV. Just below threshold, the light stop loop enhances the gluon fusion cross section. Above threshold, the rapid rise of the branching fraction of $H \rightarrow \tilde{t}_1\tilde{t}_1^*$ sharply suppresses the $H \rightarrow \tau^+\tau^-$ decay mode. Fig. 15 gives the combined limit.

Finally, we present the projected limits from SM-like Higgs searches in the small α_{eff} scenario. In order to show the importance of the $h, H \rightarrow W^+W^-$ Higgs decay channels, in Fig. 16 we present the results omitting the contributions from these channels. There is a well-known stripe of parameter space unprobed by the $b\bar{b}$ searches because of the loop-induced cancellation of \mathcal{M}_{12}^2 [23]. In Fig. 17 we present the same results, but now including the constraint from the $h, H \rightarrow W^+W^-$ channels. We find that the W^+W^- channel can cover almost all of this previously inaccessible window at 90% C.L., with sufficient improvements. In Fig. 18 we give the limit from the $\tau^+\tau^-$ channel alone.

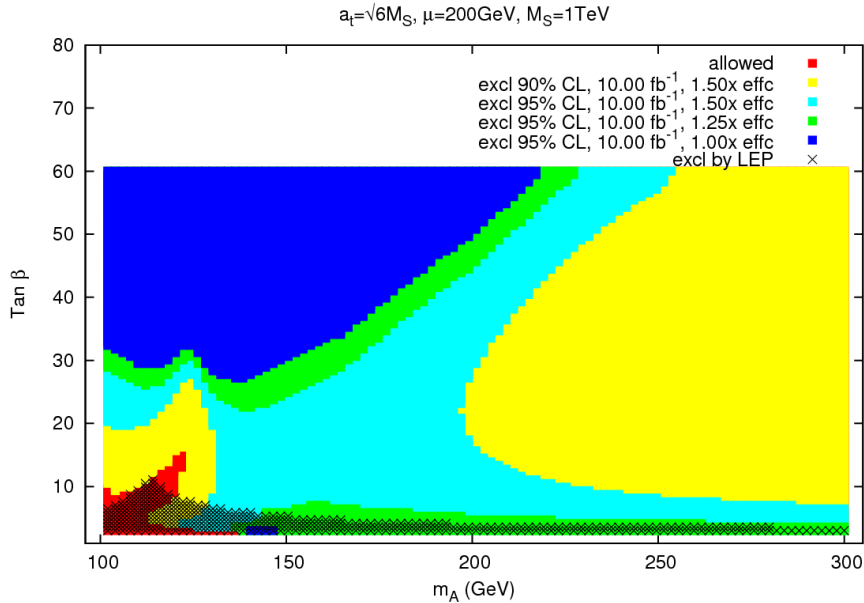


Figure 9: Exclusion limits at 90% and 95% C.L. in the maximal mixing scenario of the MSSM, including all channels.

Although it covers the region unprobed by the $b\bar{b}$ channels, it is no longer so crucial for covering all of the $(m_A, \tan \beta)$ plane, because of the limit from the W^+W^- channel. Fig. 19 demonstrates the complementarity of the searches.

7 Conclusions

In this note we have studied the improvements necessary for the Tevatron to probe the Higgs sector of the minimal supersymmetric extension of the SM. If the experiments can achieve the increases in luminosity and signal efficiency studied in this work, the Tevatron may be able to probe significant regions of the MSSM parameter space to 95% C.L., and probe all of the parameter space at 90% C.L.

In particular, if 10 fb^{-1} of integrated luminosity are achieved, a 25% increase in efficiency of the $b\bar{b}$ channel (or a similar improvement coming from the addition of other, complementary channels) will be enough to probe scenarios with small values of A_t at 95% C.L. If only 7 fb^{-1} of integrated luminosity are gathered, a 50% increase in efficiency is needed to probe these scenarios at the same level. Similar results were found in the gluophobic scenario, since the necessary light stops push the Higgs mass to low values without affecting the $b\bar{b}$ production channel in a significant way. On the other hand, if A_t acquires a larger value, close to that which maximizes the SM-like Higgs mass, both an increase in luminosity to about 10 fb^{-1} and of efficiencies by a factor 1.5 will be necessary to fully probe the MSSM Higgs sector. In addition, non-standard Higgs

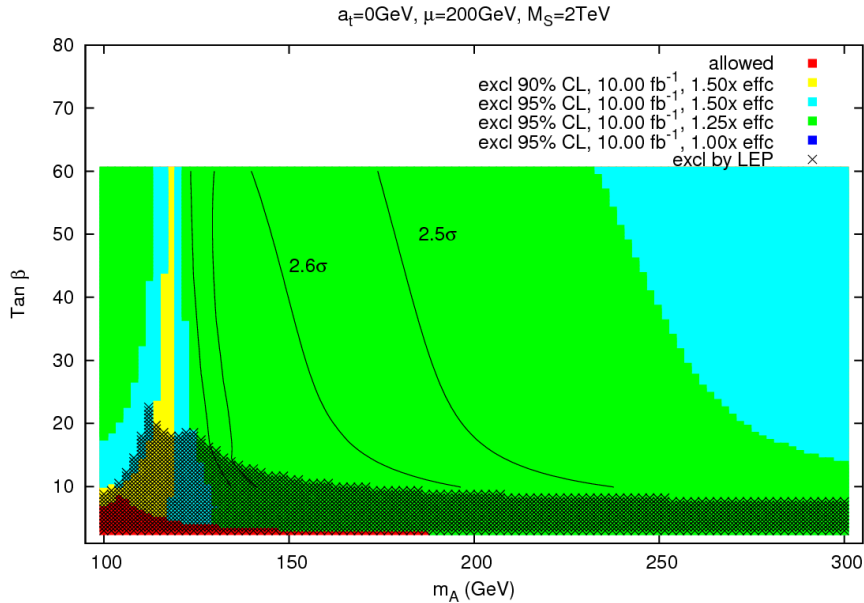


Figure 10: Exclusion limits at 90% and 95% C.L. in the no-mixing scenario of the MSSM, including only $b\bar{b}$ and W^+W^- decay channels.

searches in the inclusive $\tau^+\tau^-$ channel provide valuable complementarity to the SM-like searches in order to cover the small m_A , large $\tan\beta$ region of this scenario. Finally, the complementarity of SM-like searches in the $b\bar{b}$ and W^+W^- channels was shown to be important in scenarios in which the $hb\bar{b}$ coupling is suppressed.

Acknowledgments

Work at ANL is supported in part by the U.S. Department of Energy (DOE), Div. of HEP, Contract DE-AC02-06CH11357. Work at EFI is supported in part by the DOE through Grant No. DE-FG02-90ER40560. T.L. is also supported by the Fermi-McCormick Fellowship. This work was supported in part by the DOE under Task TeV of contract DE-FGO2-96-ER40956.

References

- [1] H. P. Nilles, Phys. Rept. **110** (1984) 1; H. E. Haber and G. L. Kane, Phys. Rept. **117**(1985) 75; S. P. Martin, arXiv:hep-ph/9709356.
- [2] H. E. Haber and R. Hempfling, Phys. Rev. Lett. **66**, 1815 (1991); Y. Okada, M. Yamaguchi and T. Yanagida, Prog. Theor. Phys. **85**, 1 (1991); J. R. Ellis, G. Ridolfi and F. Zwirner, Phys. Lett. B **262**, 477 (1991).

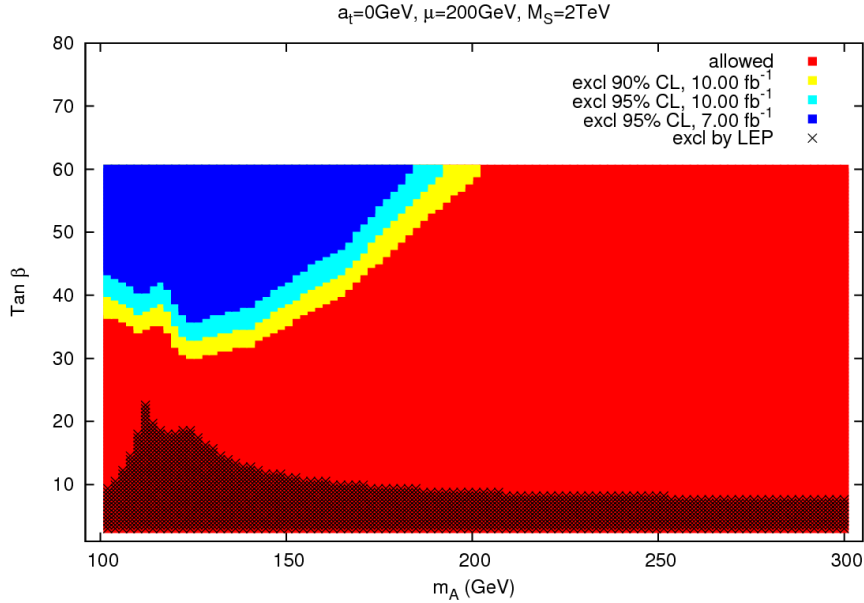


Figure 11: Exclusion limits at 90% and 95% C.L. in the no-mixing scenario of the MSSM, including only the $\tau^+\tau^-$ inclusive search. No efficiency improvements are applied.

- [3] M. S. Carena, J. R. Espinosa, M. Quiros and C. E. M. Wagner, Phys. Lett. B **355**, 209 (1995) [arXiv:hep-ph/9504316]; M. S. Carena, M. Quiros and C. E. M. Wagner, Nucl. Phys. B **461**, 407 (1996) [arXiv:hep-ph/9508343]; H. E. Haber, R. Hempfling and A. H. Hoang, Z. Phys. C **75**, 539 (1997) [arXiv:hep-ph/9609331].
- [4] S. Heinemeyer, W. Hollik, and G. Weiglein, Phys. Rev. D **58**, 091701 (1998) [arXiv:hep-ph/9803277]; S. Heinemeyer, W. Hollik, and G. Weiglein, Phys. Lett. B **440**, 296 (1998) [arXiv:hep-ph/9807423]; S. Heinemeyer, W. Hollik, and G. Weiglein, Eur. Phys. J. C **9**, 343 (1999) [arXiv:hep-ph/9812472].
- [5] J. R. Espinosa and R. J. Zhang, J. High Energy Phys. **0003**, 026 (2000) [arXiv:hep-ph/9912236]; J. R. Espinosa and R. J. Zhang, Nucl. Phys. B **586**, 3 (2000) [arXiv:hep-ph/0003246].
- [6] M. Carena, H. E. Haber, S. Heinemeyer, W. Hollik, C. E. M. Wagner, and G. Weiglein, Nucl. Phys. B **580**, 29 (2000) [arXiv:hep-ph/0001002].
- [7] G. Degrandi, P. Slavich, and F. Zwirner, Nucl. Phys. B **611**, 403(2001) [arXiv:hep-ph/0105096]; A. Brignole, G. Degrandi, P. Slavich and F. Zwirner, Nucl. Phys. B **631**, 195 (2002) [arXiv:hep-ph/0112177].
- [8] S. P. Martin, Phys. Rev. D **67**, 095012 (2003) [arXiv:hep-ph/0211366].

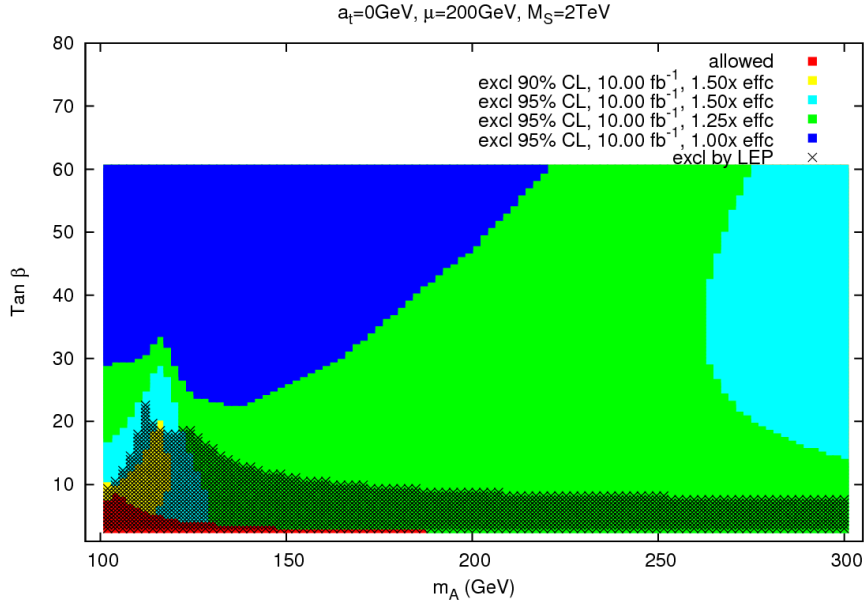


Figure 12: Exclusion limits at 90% and 95% C.L. in the no-mixing scenario of the MSSM, including all channels.

- [9] A. Stange, W. J. Marciano and S. Willenbrock, Phys. Rev. D **49**, 1354 (1994) [arXiv:hep-ph/9309294]; T. Hahn, S. Heinemeyer, F. Maltoni, G. Weiglein and S. Willenbrock, arXiv:hep-ph/0607308.
- [10] M. Spira, arXiv:hep-ph/9810289.
- [11] E. L. Berger and J. w. Qiu, Phys. Rev. Lett. **91**, 222003 (2003) [arXiv:hep-ph/0304267].
- [12] C. Anastasiou, R. Boughezal and F. Petriello, JHEP **0904**, 003 (2009) [arXiv:0811.3458 [hep-ph]].
- [13] D. de Florian and M. Grazzini, Phys. Lett. B **674**, 291 (2009) [arXiv:0901.2427 [hep-ph]].
- [14] S. Dittmaier, M. 1. Kramer and M. Spira, Phys. Rev. D **70**, 074010 (2004) [arXiv:hep-ph/0309204].
- [15] S. Dawson, C. B. Jackson, L. Reina and D. Wackerroth, Mod. Phys. Lett. A **21**, 89 (2006) [arXiv:hep-ph/0508293].
- [16] M. S. Carena *et al.* [Higgs Working Group Collaboration], arXiv:hep-ph/0010338.
- [17] T. Han and R. J. Zhang, Phys. Rev. Lett. **82**, 25 (1999) [arXiv:hep-ph/9807424].

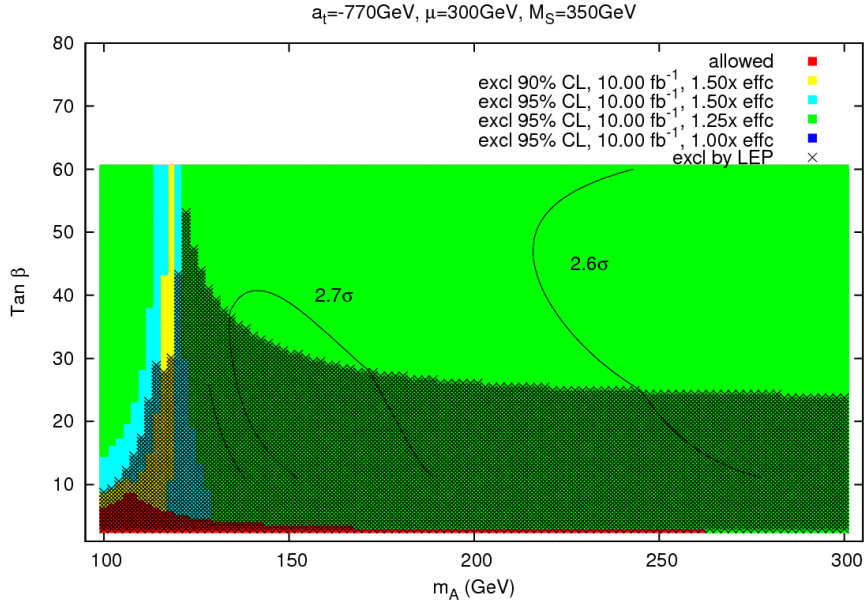


Figure 13: Exclusion limits at 90% and 95% C.L. in the gluophobic scenario of the MSSM, including only $b\bar{b}$ and W^+W^- decay channels.

- [18] T. Han, A. S. Turcot and R. J. Zhang, Phys. Rev. D **59**, 093001 (1999) [arXiv:hep-ph/9812275].
- [19] [CDF Collaboration and D0 Collaboration], arXiv:0903.4001 [hep-ex].
- [20] C. Balazs, J. L. Diaz-Cruz, H. J. He, T. M. P. Tait and C. P. Yuan, Phys. Rev. D **59**, 055016 (1999) [arXiv:hep-ph/9807349].
- [21] H. Baer, B. W. Harris and X. Tata, Phys. Rev. D **59**, 015003 (1999) [arXiv:hep-ph/9807262].
- [22] M. Drees, M. Guchait and P. Roy, Phys. Rev. Lett. **80**, 2047 (1998) [Erratum-ibid. **81**, 2394 (1998)] [arXiv:hep-ph/9801229].
- [23] M. S. Carena, S. Mrenna and C. E. M. Wagner, Phys. Rev. D **60**, 075010 (1999) [arXiv:hep-ph/9808312]; M. S. Carena, S. Mrenna and C. E. M. Wagner, Phys. Rev. D **62**, 055008 (2000) [arXiv:hep-ph/9907422].
- [24] A. Belyaev, T. Han and R. Rosenfeld, JHEP **0307**, 021 (2003) [arXiv:hep-ph/0204210].
- [25] A. Abulencia *et al.* [CDF Collaboration], Phys. Rev. Lett. **96**, 011802 (2006) [arXiv:hep-ex/0508051]; I. Kravchenko [CDF Collaboration and D0 Collaboration], in *In the Proceedings of the 15th International Conference on Supersymmetry and*

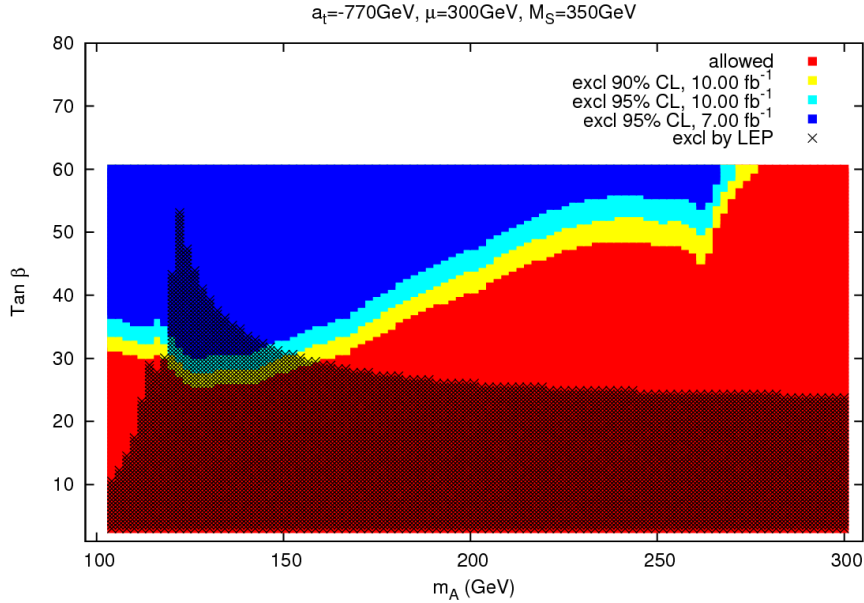


Figure 14: Exclusion limits at 90% and 95% C.L. in the gluophobic scenario of the MSSM, including only the $\tau^+\tau^-$ inclusive search. No efficiency improvements are applied.

the Unification of Fundamental Interactions (SUSY07), Karlsruhe, Germany, 26 Jul - 1 Aug 2007 arXiv:0710.5141 [hep-ex].

- [26] V. M. Abazov *et al.* [D0 Collaboration], *Phys. Rev. Lett.* **101**, 071804 (2008) [arXiv:0805.2491 [hep-ex]].
- [27] R. Hempfling, *Phys. Rev.* **D 49** (1994) 6168;
 L. Hall, R. Rattazzi and U. Sarid, *Phys. Rev.* **D 50** (1994) 7048, hep-ph/9306309;
 M. Carena, M. Olechowski, S. Pokorski and C. Wagner, *Nucl. Phys.* **B 426** (1994) 269, hep-ph/9402253.
- [28] J. A. Coarasa, R. A. Jimenez and J. Sola, *Phys. Lett. B* **389**, 312 (1996) [arXiv:hep-ph/9511402].
- [29] http://www-cdf.fnal.gov/physics/new/hdg/results/combcdf_mar09/
- [30] <http://www-d0.fnal.gov/Run2Physics/WWW/results/higgs.htm>
- [31] <http://www-d0.fnal.gov/Run2Physics/WWW/results/prelim/HIGGS/H73/>
- [32] <http://www-d0.fnal.gov/Run2Physics/WWW/results/prelim/HIGGS/H66/>
- [33] <http://www-d0.fnal.gov/Run2Physics/WWW/results/prelim/HIGGS/H59/>
http://www-cdf.fnal.gov/physics/new/hdg/results/htt_070928/index.htm

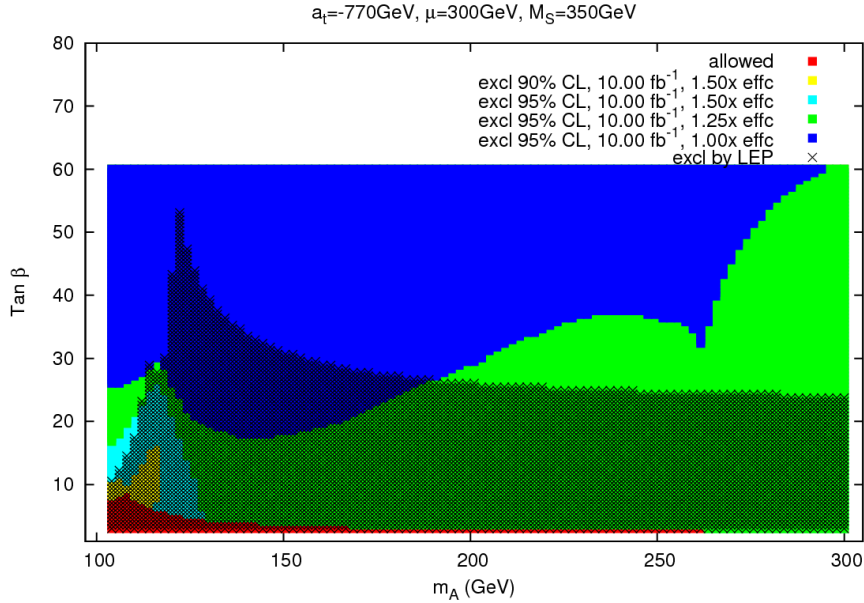


Figure 15: Exclusion limits at 90% and 95% C.L. in the gluophobic scenario of the MSSM, including all channels.

- [34] A. Djouadi, J. Kalinowski and M. Spira, *Comput. Phys. Commun.* **108**, 56 (1998) [arXiv:hep-ph/9704448].
- [35] J. S. Lee, A. Pilaftsis, M. S. Carena, S. Y. Choi, M. Drees, J. R. Ellis and C. E. M. Wagner, *Comput. Phys. Commun.* **156**, 283 (2004) [arXiv:hep-ph/0307377]; J. S. Lee, M. Carena, J. Ellis, A. Pilaftsis and C. E. M. Wagner, *Comput. Phys. Commun.* **180**, 312 (2009) [arXiv:0712.2360 [hep-ph]].
- [36] M. S. Carena, S. Heinemeyer, C. E. M. Wagner and G. Weiglein, *Eur. Phys. J. C* **26**, 601 (2003) [arXiv:hep-ph/0202167].
- [37] [Tevatron Electroweak Working Group and CDF Collaboration and D0 Collab], arXiv:0903.2503 [hep-ex].
- [38] A. Sopczak [ALEPH Collaboration and DELPHI Collaboration and L3 Collaboration and], arXiv:hep-ph/0602136.
- [39] A. Djouadi, *Phys. Lett. B* **435**, 101 (1998) [arXiv:hep-ph/9806315].
- [40] A. Menon and D. E. Morrissey, arXiv:0903.3038 [hep-ph].
- [41] M. S. Carena, S. Heinemeyer, C. E. M. Wagner and G. Weiglein, *Eur. Phys. J. C* **45** (2006) 797 [arXiv:hep-ph/0511023].

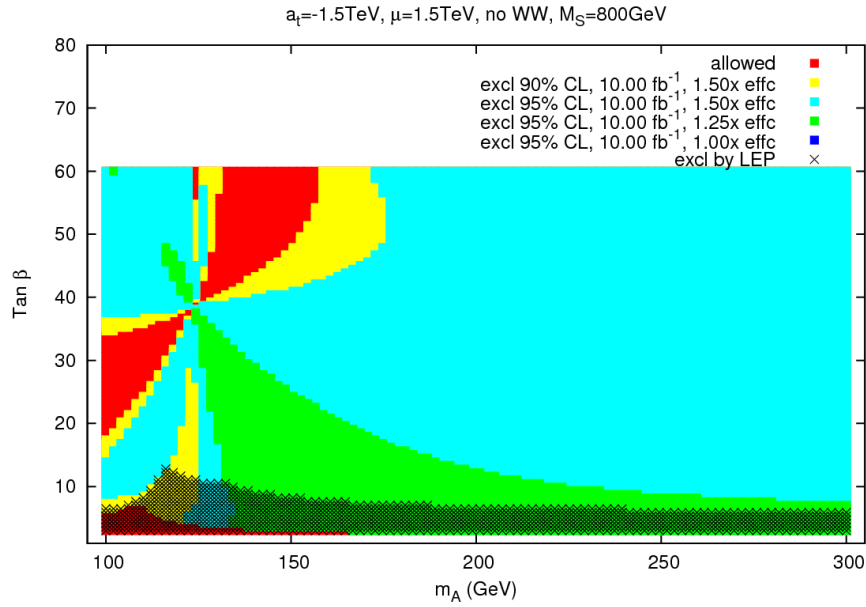


Figure 16: Exclusion limits from the $h, H \rightarrow b\bar{b}$ channels at 90% and 95% C.L. in the small α_{eff} scenario of the MSSM.

[42] L. Roszkowski, R. R. de Austri and R. Trotta, JHEP **0704**, 084 (2007) [arXiv:hep-ph/0611173].

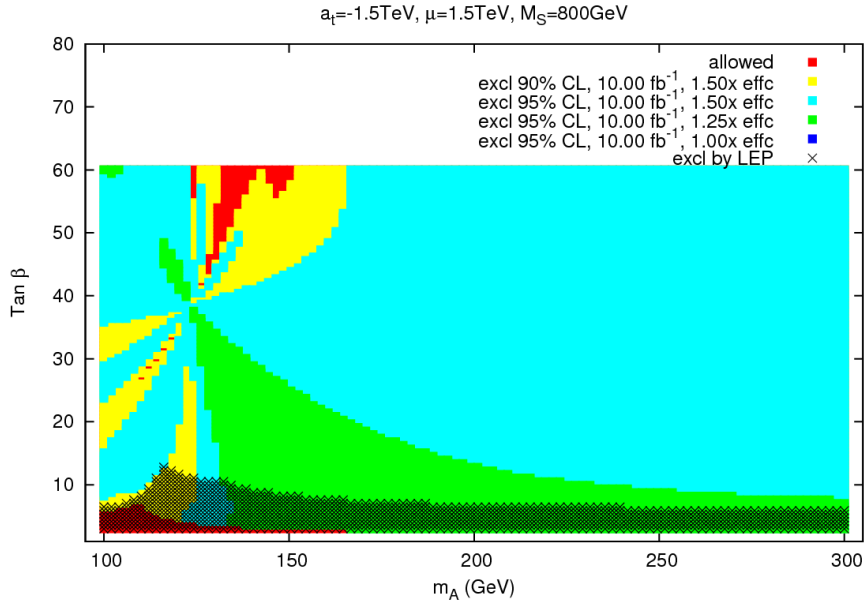


Figure 17: Exclusion limits from the $h, H \rightarrow b\bar{b}$ and $h, H \rightarrow W^+W^-$ channels at 90% and 95% C.L. in the small α_{eff} scenario of the MSSM.

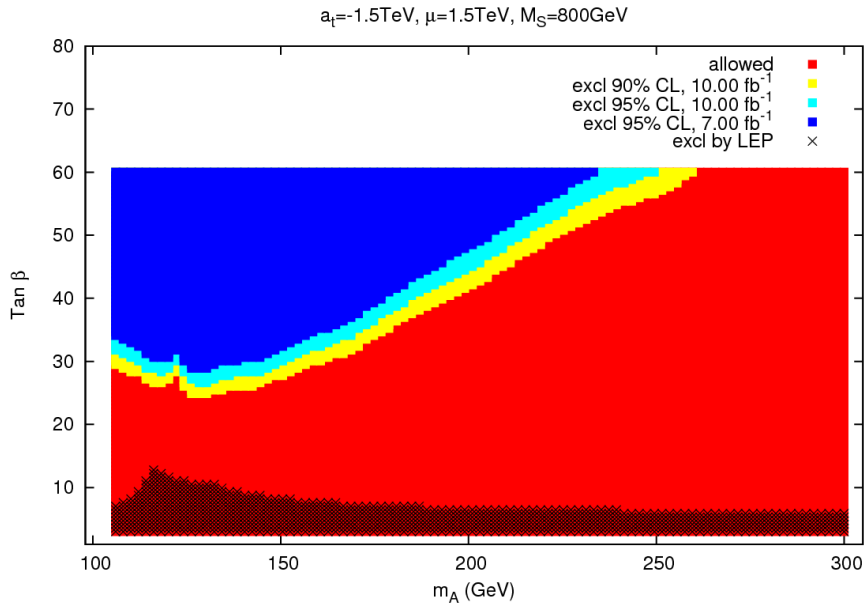


Figure 18: Exclusion limits at 90% and 95% C.L. in the small α_{eff} scenario of the MSSM, including only the $\tau^+\tau^-$ inclusive search. No efficiency improvements are applied.

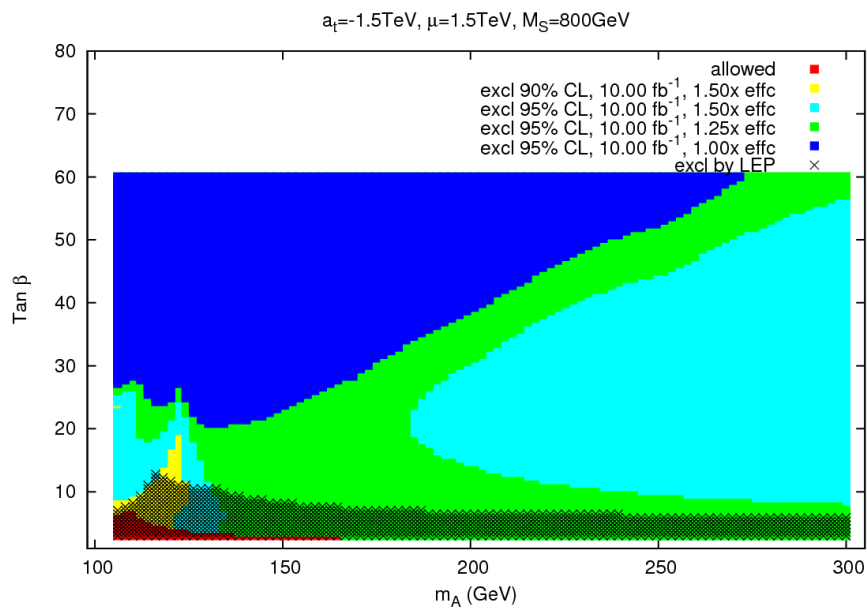


Figure 19: Exclusion limits at 90% and 95% C.L. in the small α_{eff} scenario of the MSSM, including all channels.